

Proceedings of the Fifth Annual LHCP

July 23, 2018

Using leptons p_T measurements to constrain Z' -bosons widths in Drell-Yan processes at the LHC

JURI FIASCHI, ELENA ACCOMANDO, STEFANO MORETTI, CLAIRE H. SHEPHERD-THEMISTOCLEOUS¹

*Department of Physics and Astronomy
University of Southampton, United Kingdom*

ABSTRACT

We recognise the appearance of a Focus Point (FP) in the transverse momentum distribution of either leptons originating from a BSM Z' -boson decay, after a simple normalisation procedure. Exploring the properties of the FP we will be able to define in a general way a new observable, the Focus Point Asymmetry (A_{FP}), which can be used to set constraints on the Z' width. We discuss the potential and the sensitivity of the A_{FP} as a diagnostic tool for Z' physics, considering various Z' phenomenological realisations.

PRESENTED AT

The Fifth Annual Conference
on Large Hadron Collider Physics
Shanghai Jiao Tong University, Shanghai, China
May 15-20, 2017

¹Work supported by the Science and Technology Facilities Council, grant number ST/L000296/1. All authors acknowledge partial financial support through the NExT Institute.

1 Introduction

The recent upgrade in energy of the LHC is unfolding the high invariant mass region looking for any hint of BSM physics. At the same time, the steady increase of integrated luminosity is building a very large data set, which requires sharp analysis techniques to disentangle new physics signals.

A common prediction of many BSM scenarios is the appearance of an additional massive neutral gauge boson in the spectrum, often called a Z' . The golden channel for the detection of a Z' -boson is the opposite-charge same-flavour two-lepton final state. Its signal would appear as a peak in the invariant mass distribution of the di-lepton pair, following the shape of a Breit-Wigner (BW) functional form. Phenomenologically, Z' 's can appear in a large variety of realisations. The most common scenario would be a narrow peak ($\Gamma_{Z'}/M_{Z'} \sim 1\%$) standing over a null background. In this picture, the traditional experimental searches based on the “bump” hunt strategy have maximal sensitivity and from the absence of new physics evidences, lower bounds on the Z' mass can be extracted in a model independent way [6], such that their re-interpretation in other frameworks is unambiguous. With this approach the ATLAS [2] and CMS [3] collaborations regularly release updated bounds, exploiting the latest available data. The most recent results set the mass of the Z' -boson to $M_{Z'} > 4$ TeV for the most of the single Z' benchmark models (4.5 TeV for the SSM) [2].

The purpose of this article is to introduce a novel observable which can be used to support the analysis of a signal coming from a BSM Z' -boson [4]. We will consider the transverse momentum distribution of either lepton in the final state. We will highlight the appearance of a Focus Point (FP) carrying interesting model independent features and exploiting those properties we will define a new observable and finally we will examine its discovery and diagnostic potential, especially in the unfriendly scenario of broad Z' resonances.

2 The Focus Point and its properties

As mentioned in the previous section, the current lower bounds on the mass of narrow Z' -bosons is around 4 TeV [2]. However, those limits apply only if the resonance is narrow, such that the method used to extract those limits breaks down if the resonance width is enhanced $\Gamma_{Z'}/M_{Z'} > 5\%$ [4]. There exist many physical situations where this condition is satisfied. In particular, a mixing in the neutral sector, or the opening of new exotic decay channels for the Z' resonance, serve this purpose [?, ?]. In essence, the minimal realisations of narrow Z' 's and their conventional analysis based on the “bump” hunt, although being a necessary first step in the quest for detecting new physics signals, usually only covers a small part of the parameter space of a specific model and in general does not include all the possible phenomenological scenarios.

In the following we will consider Z' signals beyond the narrow width approximation. In particular, we will refer to some single Z' constructions that are usually adopted as benchmarks models and we will modify the Z' width by hand, which means that the fermions couplings will not be changed (production cross section unchanged), while the partial decay branching ratios will be rescaled (following the inverse of the width). Within this parametrisation, we are going to consider also resonances with masses on the edge of the exclusion limits (or sometimes below), only with the purpose of comparing their signal shape with their unexcluded counterparts featuring an enhanced width. We are also presenting our analysis in the High Luminosity Large Hadron Collider (HL-LHC) setup, as the diagnostic features of the new observable we are introducing will be exploited in this regime.

2.1 Profiling Z' signals in the di-lepton channel

The profile of a Z' resonance in the di-lepton invariant mass spectrum is visible in Fig. 1(a), where three popular benchmarks have been selected, the E6-I model, the Left-Right Symmetric model (LR) and the Sequential Standard Model (SSM), fixing the resonance mass at $M_{Z'} = 4$ TeV and its width at $\Gamma_{Z'}/M_{Z'} = 1\%$. We are considering an integrated luminosity of $\mathcal{L} = 1$ ab $^{-1}$, such that, in this case of narrow resonances, the peaks are very visible with a moderate statistics. As the resonance width grows, the sensitivity on the BW peak decreases rapidly. In Fig. 1(b) we are considering one benchmark model (the SSM) with the Z' mass fixed at $M_{Z'} = 4$ TeV, while its width over mass ratio varies between 1% and 20%. Already for

$\Gamma_{Z'}/M_{Z'} > 5\%$, the number of events drops sensibly and the “bump” hunt strategy fails in detecting the resonance.

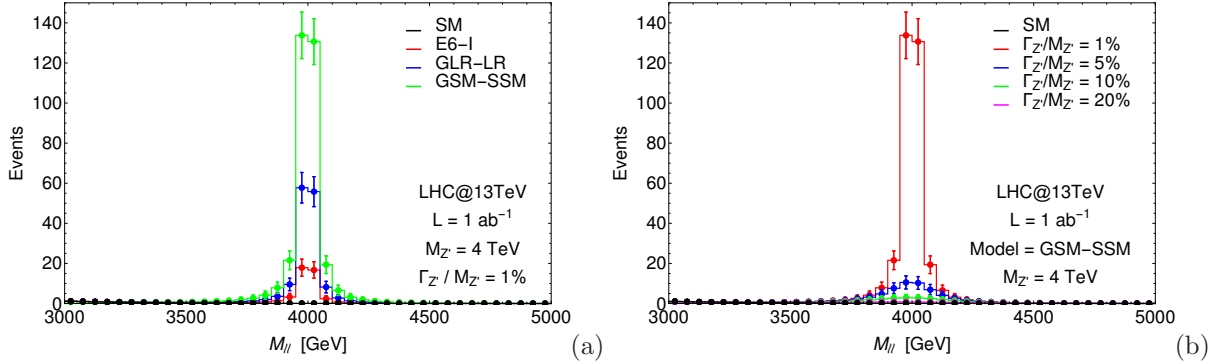


Figure 1: Distribution of number of events as function of the di-lepton invariant mass as predicted in the SM and (a) and in three Z' benchmark models fixing the width of the resonance at 1% of its mass (b) and in the SSM fixing the width of the resonances at four different values (1%, 5%, 10% and 20% of the mass) and $M_{Z'} = 4$ TeV, for the 13 TeV LHC and with $\mathcal{L} = 1$ ab^{-1} . Acceptance cuts are applied ($|\eta| < 2.5$), detector efficiencies are not accounted for.

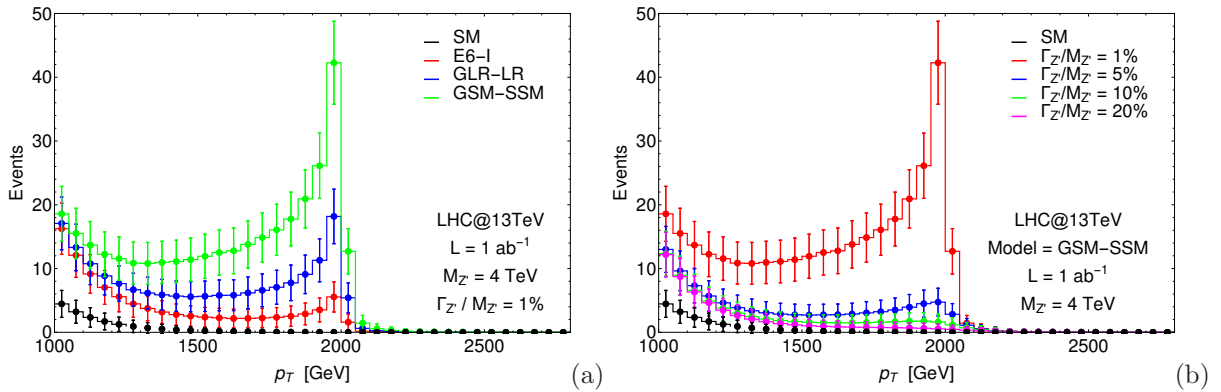


Figure 2: Same as Fig. 1 for the distributions of number of events as function of the p_T of either lepton.

Consider now the transverse momentum distribution of either lepton in the final state. The p_T distributions of the number of events in the corresponding case of Fig. 1 are visible in Fig. 2. The Jacobian peaks in Fig. 2(a) are well visible, but observing Fig. 2(b) it is clear that a shape analysis of a resonance with $\Gamma_{Z'}/M_{Z'} > 5\%$ would be a difficult task.

2.2 The Focus Point

The first step towards the definition of the new observable consists in normalising the curves of Fig. 2.

The result is visible in Fig. 3 where the normalisation interval of each curves has been fixed between a $p_T^{\min} = 1000$ GeV, and a p_T^{\max} that can be chosen at any value sufficiently far from the Jacobian peak at $M_{Z'}/2$ to consider all the available data. The interesting feature appearing from Fig. 3 is that now all the curves cross through the same point, that we will call Focus Point (FP).

The FP shows remarkable qualities, already visible in these plots. In Fig. 3(a) we can see that its position is model independent while from Fig. 3(b) we can recognise that is also independent of the resonance width. It is also to notice that the SM background as well crosses the FP.

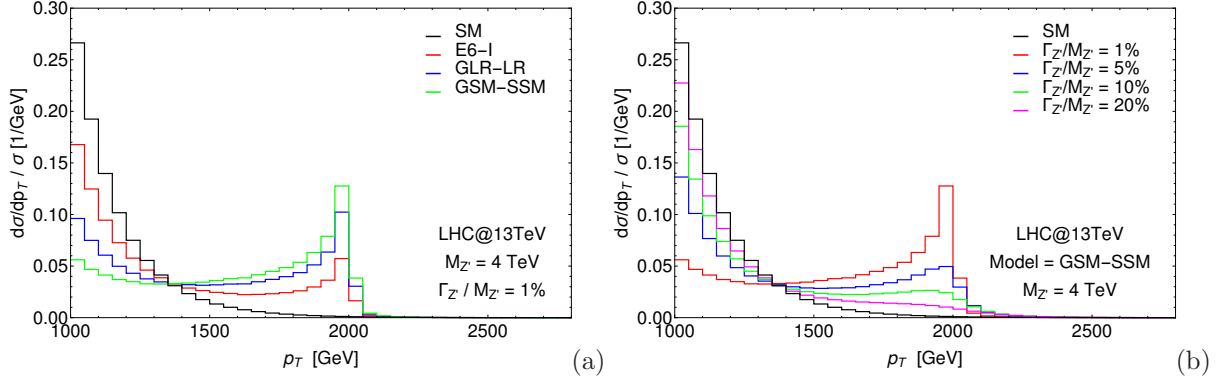


Figure 3: Normalized distribution obtained from Fig. 2 with $p_T^{\min} = 1000$ GeV.

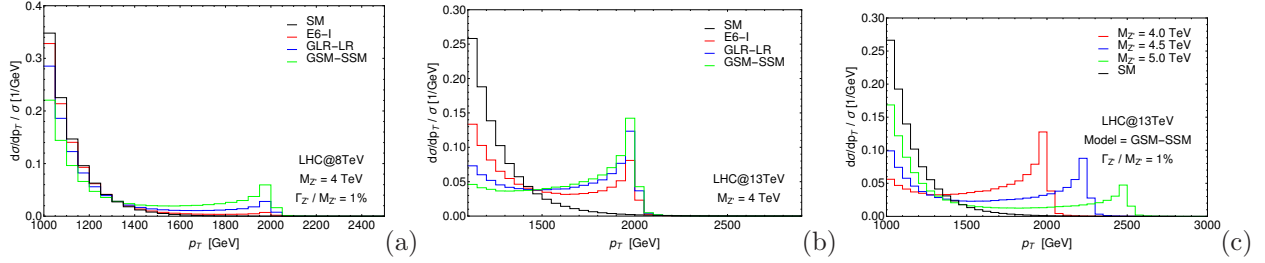


Figure 4: Normalised p_T distribution of either lepton as predicted in the SM and in the three benchmarks fixing $M_{Z'} = 4$ TeV and $\Gamma_{Z'}/M_{Z'} = 1\%$, in the same setup as before but changing (a) the LHC collider energy to 8 TeV, (b) the $p_T^{\min} = 1100$ GeV, and (c) in the SSM fixing the Z' mass to 4, 4.5 and 5 TeV.

The position of the FP indeed depends only on few parameters, that are summarised in Fig. 4. In Fig. 4(a) we changed the collider energy to 8 TeV and the FP consequently changed. Anyway from now on we will consider only the setup of the LHC at 13 TeV, as this is and will be the environment of current and future analysis. It has been verified [4] that the effects of kinematical cut (such as $|\eta|$ acceptance cuts) as well as interference effects are totally irrelevant in our analysis and they do not affect the appearance of the FP, neither they spoil any of its features.

Fixing the collider centre-of-mass energy, we have noticed that the position of the FP is then determined only from two parameters which are the choice of the p_T^{\min} and the mass of the Z' . An empirical relation has been derived from the results of the simulations:

$$FP = p_T^{\min} + 10\%M_{Z'}. \quad (1)$$

Since the FP arises from the normalisation procedure defined above, it is by all means determined by the choice of the p_T^{\min} , assuming the above condition on the p_T^{\max} . In Fig. 4(b) the lower limit on the normalisation has been fixed to $p_T^{\min} = 1100$ GeV and the position of the FP has scaled accordingly to Eq. 1. The other relevant parameter to the FP position is the Z' mass, that we have varied in Fig. 4(c) between 4 and 5 TeV, which is the $M_{Z'}$ region that will be covered in ongoing analysis. Again the position of the FP, that now can be identified by the crossing point between the SM and BSM curves, follows the empirical relation derived in Eq. 1.

3 The Asymmetry of the Focus Point

Now consider the interval in the p_T spectrum that has been chosen for the above normalisation. The FP can be used to separate the interval in two regions, on the “left” and on the “right” side of the FP. We define the L and R quantities as the integrals of the curves of Fig. 3 in the two corresponding subregions:

$$L = \frac{1}{N} \int_{p_T^{\min}}^{\text{FP}} \frac{d\sigma}{dp_T} dp_T, \quad R = \frac{1}{N} \int_{\text{FP}}^{p_T^{\max}} \frac{d\sigma}{dp_T} dp_T. \quad (2)$$

The new observable that will be called Asymmetry of the Focus Point (or A_{FP}) is defined as the normalised difference between these two integrated quantities:

$$A_{\text{FP}} = \frac{L - R}{L + R}. \quad (3)$$

For a given resonance (*i.e.* a Z' with a fixed mass and width) the A_{FP} only depends on the choice of the p_T^{\min} by construction. In the situation where a Z' signal is observed, the new observable can be used to support the evidence and its measurement provides an independent information on the underlying model generating the new boson and more importantly on the width of the resonance.

In order to test the sensitivity of the A_{FP} , in each plot of Fig. 5 we are showing its value and its statistical error for different choices of the resonance width, as function of the choice of the p_T^{\min} (the value that has been used for the position of the FP follows Eq. 1). This is repeated for three benchmark models (E6-I, LR and SSM), each time for two different values of the Z' mass and integrated luminosity (4 TeV with $\mathcal{L} = 1 \text{ ab}^{-1}$ and 5 TeV with $\mathcal{L} = 3 \text{ ab}^{-1}$). As visible comparing Fig. 5(a), (c) and (e), or the corresponding plots with $M_{Z'} = 5 \text{ TeV}$, if we assume to know the mass of the resonance (easily inferable from the invariant mass distribution) and its width, a measurement of the A_{FP} can be useful to disentangle the underlying BSM model. However the three benchmark models chosen here are representative of their respective classes (E6, Generalised Left-Right or GLR and Generalised Standard Model or GSM), in the sense that it has been verified [4] that the value of the A_{FP} is similar for each model within the same class, such that the observable is able to distinguish between different classes of models, but has almost no sensitivity in distinguishing the particular model within each class.

More importantly is the case where we fix the BSM construction and the Z' mass, while we seek for information on the resonance width. This would be a common scenario imagining that a Z' peak is observed and various benchmark models would be used to fit the signal. In this framework the A_{FP} can be used to derive important constraints on the resonance width, which can be imported as independent constraint in the experimental fit of the BW shape in the invariant mass spectrum. As visible in Fig. 5 the A_{FP} can constrain resonance widths up to $\Gamma_{Z'}/M_{Z'} = 5\%$, $\Gamma_{Z'}/M_{Z'} = 10\%$ and $\Gamma_{Z'}/M_{Z'} = 20\%$ respectively within the E6, GLR and GSM classes of models.

4 Conclusions

We have introduced a new observable, the A_{FP} that can be used for Z' diagnostic in the di-lepton final channel. The definition of the novel observable goes through simple measurements on the transverse momentum spectrum of either lepton in the final state.

We have shown that a FP appears once normalising the p_T distributions obtained for various Z' benchmark models with different widths and for the SM. The position of the FP indeed does not depend on the underlying BSM construction neither on the resonance width. By construction it only depends on the Z' mass and on the p_T^{\min} , which defines the interval chosen for the normalisation (once we assume $p_T^{\max} > M_{Z'}/2$). We have derived an empirical relation between the position of the FP, the mass of the Z' and the chosen p_T^{\min} , which holds for the LHC with 13 TeV c.o.m. energy and for the $M_{Z'}$ parameter region of concern during the Run-II and the HL-LHC stage.

Exploiting the FP and its properties, we have defined the A_{FP} observable as the normalised difference between two (normalised) differential cross sections integrated in two regions of the p_T spectrum separated

by the FP. As already said, the position of the latter is both model and width independent, thus assuming to have a fixed collider energy and the value of the Z' mass from invariant mass measurements, the A_{FP} observable is well defined and its measured value will depend only on the choice of the p_T^{min} and on the resonance width.

Being an integrated observable, the A_{FP} exploits the full data set and its statistical uncertainty is therefore small, and consequently it also does not require any modelling of the shape. Moreover, being a ratio of cross sections, part of the systematic uncertainties affecting the A_{FP} naturally cancel. In this sense it can be useful to support the diagnostic analysis of an excess of events observed in the di-lepton high invariant mass, as it provides independent constraints on the Z' width, that can improve the quality of experimental fits. The properties we have described for the A_{FP} make it a very attractive search tool as well, as it still maintain a good sensitivity on new physics also in the problematic context of broad resonance detection.

References

- [1] E. Accomando, D. Becciolini, A. Belyaev, S. Moretti and C. Shepherd-Themistocleous, JHEP **10**, 153 (2013) [arXiv:1304.6700 [hep-ph]].
- [2] [ATLAS Collaboration], ATLAS-CONF-2017-027 (2017) [<http://cds.cern.ch/record/2259039>].
- [3] [CMS Collaboration], CMS-PAS-EXO-16-031 (2016) [<http://cds.cern.ch/record/2205764>].
- [4] E. Accomando, J. Fiaschi, S. Moretti and C. Shepherd-Themistocleous, [arXiv:1703.04360 [hep-ph]].
- [5] W. Abdallah, J. Fiaschi, S. Khalil and S. Moretti, JHEP **02**, 157 (2016) [arXiv:1510.06475 [hep-ph]].
- [6] E. Accomando, C. Coriano, L. Delle Rose, J. Fiaschi, C. Manzo and S. Moretti, JHEP **07**, 086 (2016) [arXiv:1605.02910 [hep-ph]].

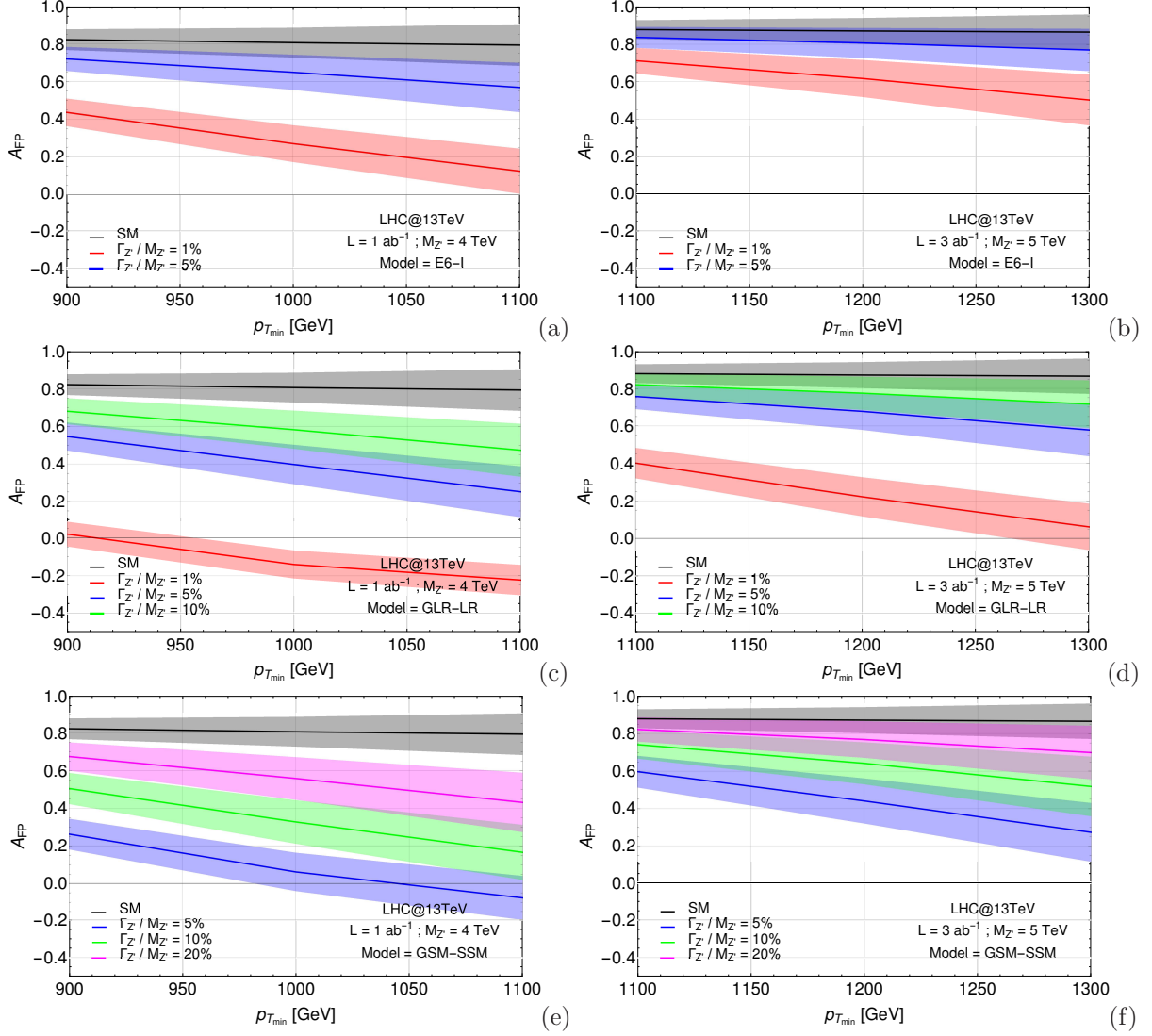


Figure 5: A_{FP} central value and statistical 1σ error band as function of p_T^{\min} cut for the LHC at 13 TeV and $\mathcal{L} = 1 \text{ ab}^{-1}$. The black line represents the SM while the coloured lines represent four different widths (1%, 5%, 10% and 20%) of the Z' resonance in the (a) E6-I, (c) GLR-LR and (e) GSM-SSM model fixing $M_{Z'} = 4 \text{ TeV}$. Same exercise is repeated in (b), (d) and (f) fixing $M_{Z'} = 5 \text{ TeV}$ and $\mathcal{L} = 3 \text{ ab}^{-1}$. The values of the FP are chosen in accordance to Eq. 1.